Chapter 2

Materials and Methods

I. MATERIALS

2.1 GENERAL INFORMATION ON THE STUDY CATCHMENT

The objective of this thesis, as mentioned earlier, is to assess the role of various lithological units in contributing to the major ions, Sr and Re budgets and Sr isotope systematics of the Yamuna River System (YRS) in the Himalaya and to evaluate the role of silicate vs. carbonate weathering on the Sr isotopic composition of the river waters. This study also focuses on CO_2 consumption rates associated with silicate weathering in the YRS and the Ganga basins in the southern slopes of the Himalaya. To achieve these goals, it is necessary to have information and knowledge on weathering of silicates, sources of protons contributing to it and factors controlling chemical weathering such as general geology, climate and vegetation of the catchment. This chapter provides details on broad lithology and geohydrology of the Yamuna basin, sampling methods and analytical techniques employed for measurements of various parameters.

The Yamuna though rises in the Higher Himalaya, a significant part of its drainage is contained in the Lesser Himalaya. The Main Central Thrust (MCT) demarcates the boundary between the Lesser and the Higher Himalaya in the north whereas the Main Boundary Thrust (MBT) defines the boundary between the Lesser Himalaya and the Siwaliks in the south (Gansser, 1964). The Higher Himalaya is characterized by tectonically active topography, comprising of very thick piles of Precambrian high-grade metamorphics and granitic gneisses, the oldest rocks of the Himalaya (Valdiya, 1980; 1998) known as Higher Himalyan Crystallines (HHC).

The Lesser Himalaya, covering a zone of 60 to 100 km wide in between the Siwaliks and the Higher Himalaya, represents a relatively gentle and mature topography with gentle slopes and deeply dissected valleys which bear the evidences of recent rejuvenation (Valdiya, 1980). On an average the elevation ranges from 1500 m in the valley beds to 2700 m along the crest of the ridges (Devi, 1992). The Lesser Himalaya comprises of Precambrian-Paleozoic sedimentary strata with minor occurrences of displaced crystallines (Valdiya, 1980). The sedimentaries are divided in to two NW-SE elongated sequences by the crystalline klippe lying in between. The northern sequence of Precambrian sedimentaries is known as the *inner belt* whereas the southern part, known as the *outer belt,* contains sediments of possible Paleozoic age (Valdiya, 1980). The folded autocthonous sedimentaries

of the inner belt are divided into the Damtha and Tejam Groups. The Damtha Group, consisting of the Chakrata and Rautgara Formations is conformably overlain by the Tejam Group comprising the Deoban (≈Shali) and Mandhali (Sor) Formations. The sedimentary successions of the outer belt is divided into the Blaini, Infra-Krol, Krol and the Tal Formations, together known as the Krol Belt.

Fig. 2.1 Map of India The Ganga and the Yamuna from their origin in the Higher Himalaya to their confluence.

Siwaliks form the southern front of the Himalaya. These are made up of sediments deposited by the ancient Himalayan rivers in their channels and floodplains. There are flat stretches within the otherwise rugged Siwalik terrane called the "duns" consisting of gravelly deposits in depressions of now vanished lakes that were formed in the synclinal valleys (Valdiya, 1998).

The drainage basins of the Yamuna and its tributaries in their upper reaches in Himalaya cover the northwestern part of the Uttaranchal State (Figs. 2.1, 2.2). They flow through various formations in the Lesser Himalaya comprising diverse lithology set in complex stratigraphic position due to the faulting and thrusting activities. The following

section provides a compilation of the available information on the lithology drained by the Yamuna and its tributaries. Much of the information given below is drawn from Valdiya (1980).

2.1.1 Major rivers of the Yamuna River System in the Himalaya

The Yamuna

The Yamuna originates in the Yamunotri Glacier at the base of the Bandarpunch peak in the Higher Himalaya (Negi, 1991). The glacial lake of Saptarishi Kund, near the Kalind Mountain, at an altitude of 4421 m, is the source of the river. The Yamuna runs almost parallel to the Ganga till it joins the latter at Allahabad. Among all the tributaries of the Ganga, the Yamuna has the largest drainage area and stands second in terms of water discharge. It receives waters from glacier/snow melt in the source region, from monsoon rains and from springs and various tributaries along its course downstream. The Yamuna has a number of tributaries in the Himalaya, prominent among them are the Tons, Giri, Aglar, Asan and Bata. Near its source in the Higher Himalaya, the Yamuna drains mainly the crystallines of Ramgarh and Almora Groups (Fig. 2.3). The Almora granites, at their northern

Fig. 2.2 Yamuna River in its upper reaches. Also shown are the Bhagirathi and the Alaknanda and the major towns in the Yamuna River Basin.

border, are reported to have graphitic horizons of schistose graphitoid quartzites (Gansser, 1964). The metamorphics in the Almora and Ramgarh Groups have occurrences of graphitic/carbonaceous schists and carbonaceous schist-marble alternations (Valdiya, 1980). Occurrences of calc-schists and marble with sulphide mineralization have been reported in the areas upstream of Hanuman Chatti (Jaireth et al, 1982). From the Higher Himalaya the Yamuna flows in the southwest direction and enters the Lesser Himalaya where it drains a variety of lithologies. These will be described in their order as the Yamuna flows downstream. Past the Higher Himalaya, it flows through a large stretch of massive sericitic quartzite of Berinag Formation surmounted by patches of muddy quartzites, conglomerates and purple slates of Rautgara Formation. The river then drains the Barkot units comprising carbonaceous schistose phyllites intruded by dolerite sills near Barkot and chloritic phyllite with subordinate metasiltstone and quartzite near Naugaon (Valdiya, 1980). Downstream, it passes through the massive dolomitic limestone and marble of Mandhali and Deoban Formations associated at places with carbonaceous and grey slate. The Yamuna then enters a large stretch of the sedimentaries of the Chakrata Formation which constitute purple and green micaceous greywacke interbedded with slate and siltstone. Further downstream, it drains Chandpur Formation comprising of phyllites and phyllitic slates alternating with metagreywacke and metasiltstones; Nagthat Formation comprising purple and green sercitic quartzites with subordinate slates and siltstones and Bani-Subathu Formations which constitute oolitic and shelly limestones and flysch-like sediments. Barites occur in the silisiclastic sediments of Nagthat Formations in the Tons river section (Sachan and Sharma, 1993) and in the lower horizons of Krol limestones at Maldeota and Shahashradhara, where they occur as pockets and veins (Anantharaman and Bahukhandi, 1984). Southwest of Kalsi, the Yamuna enters the Siwaliks comprising the channel and floodplain deposits by the Himalayan rivers in the past.

In the Lesser Himalaya, occurrences of grayish black, black and bleached shales are reported in the Infra Krol the Lower Tal, the Deoban and the Mandhali Formations (Gansser, 1964; Valdiya; 1980). These are exposed at a number of locations in the Yamuna and the Tons catchment, the largest being at Maldeota and Durmala, around Dehradun, where phosphorite is mined economically.

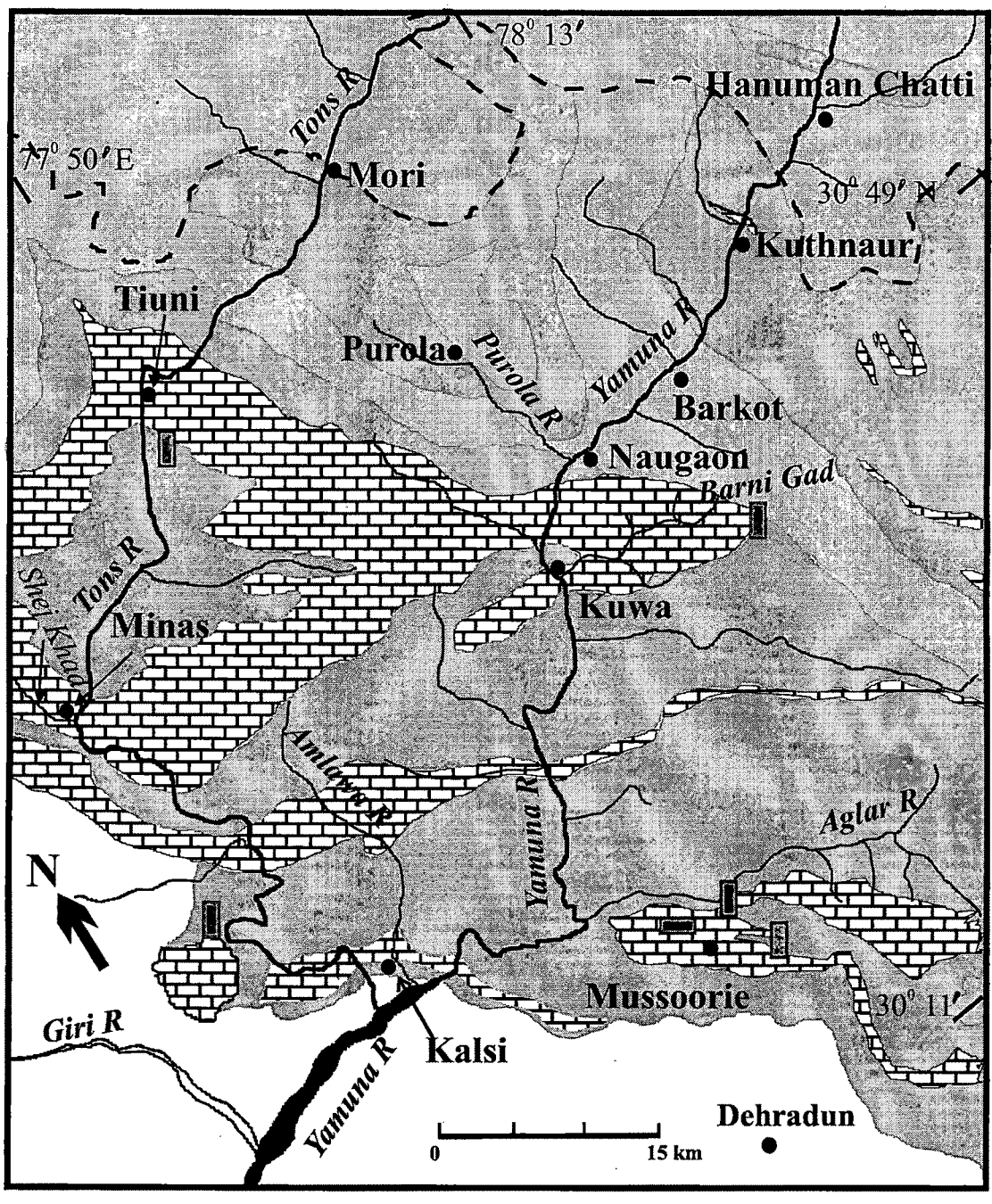

Fig. 2.3 Lithology map of the Yamuna catchment in the Himalaya

Gypsum occurs in Krol Formation in the form of pockets and bands (Anantharaman and Bahukhandi, 1984; Valdiya, 1980). Near Shahashradhara, gypsum is found as replacement deposits in the upper Krol dolomitic limestones and is economically workable. Geothermal springs occur mainly in and around the source region, in Yamunotri and Janaki Chatti.

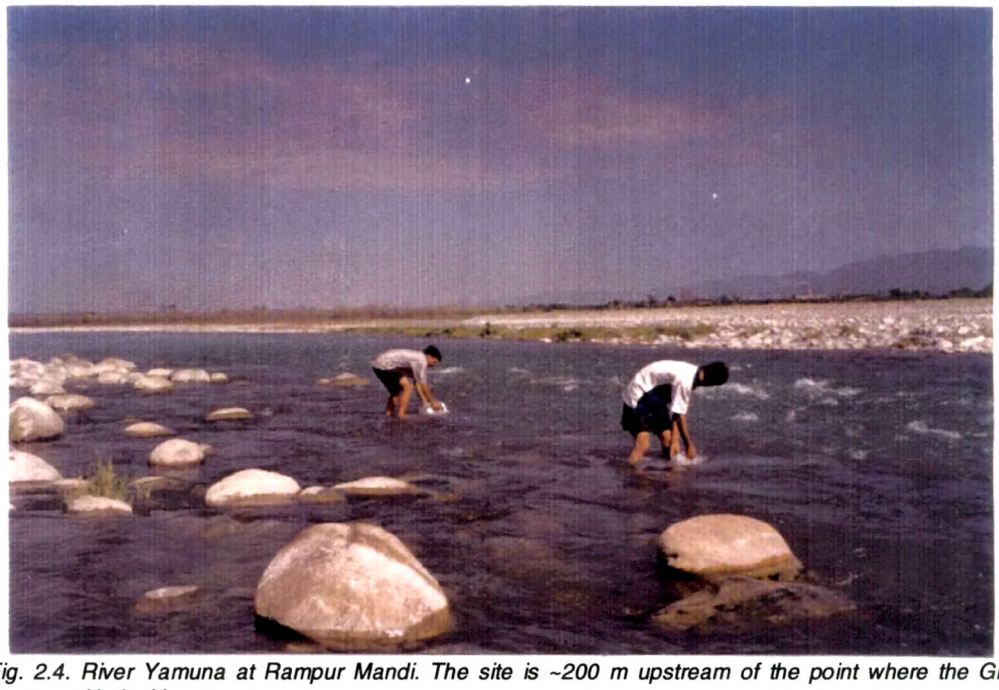

Fig. 2.4. River Yamuna at Rampur Mandi. The site is ~200 m upstream of the point where the Gin merges with the Yamuna.

The Yamuna has been dammed at Dakpathar, 6 km downstream of Kalsi. Alpine, sub-alpine, temperate and sub-tropical vegetation covers the Yamuna catchment. The main human settlements along the river are Yamunotri, Hanuman Chatti, Barkot, Naugaon, Kalsi, Vikasnagar and Paonta.

The Tons

The Tons River is the major tributary of the Yamuna. It takes its name at Naitwar, where the two rivers, the Supin and the Rupin originating in the Higher Himalaya and draining predominantly the Almora Crystallines merge together (Negi, 1991). Hereafter, the Tons flows a large distance along the border of Himachal Pradesh and Uttaranchal before merging with the Yamuna at Kalsi. The Tons, along its course, drains similar types of lithology as described for the Yamuna. In its catchment, black shales occur in areas around Tiuni and Lokhandi area on the Chakrata-Tiuni road. It joins the Yamuna at Kalsi, where it carries twice the water that is carried by theYamuna (Rao, 1975).

Its catchment bears some of the densest forests in the western Himalaya. These are primarily birch, fir, spruce, blue pine, chir pine and moru oak forests. The settlements along the river are Naitwar, Tiuni and Minas.

The Aglar

The river Aglar originates as a number of small streams fed by groundwater on the western slope of the ridge separating the drainage of the Yamuna and the Bhagirathi (Negi, 1991). Thereafter it flows in western direction to join the Yamuna at a place called Yamuna Bridge. The streams draining the limestones and slates of the Krol Formation in the northern slopes of the Mussorie Ridge and conglomerates, grey phyllitic slates and carbonaceous pyritous slate of Blaini Formation contribute water to the Aglar. The slates of the Krol Formation in the Aglar valley are iron-stained and black carbonaceous (Valdiya, 1980). The Krol dolomitic limestones in this area have pockets of gypsum and intercalations of green and grey pyritic slates (Valdiya, 1980). In its course, it also drains dirty quartzites with intercalations of siltstones and slates of Nagthat Formation and green and grey carbonaceous phyllites of Chandpur Formation alternating with greywacke. Pebbles of black shales were found in the riverbed of the Aglar during the water and bedrock sampling.

The Giri

The Giri River originates near Shimla as a spring fed by ground water and flows along the northern base of the Nahan ridge in its lower course and joins the Yamuna near Paonta Sahib (Negi, 1991). It drains conglomerates, sandstones, siltstones, quartzites, phyllites, carbonaceous and pyritiferous shales and slates with interbeded of limestones of Simla and Jaunsar Group, lithology of the Tal, Krol and Blaini Formations (Srikantia and Bhargava, 1998).

The Asan

Two spring-fed streams emanating from the limestone caves of the Mussoorie ridge merge to form the Asan River which flows south-west to join the Yamuna near Herbettpur (Negi, 1991). In its lower reaches it drains predominantly the Siwaliks. Broad river terraces developed along the middle and lower courses of the river are under cultivation. Sub tropical forests occur in the upper catchment of the river.

The Bata

The river Bata originates in the boulder below the Nahan ridge in Himachal Pradesh as the Jalmusa-ka-khala fed by rainwater and joins the Yamuna downstream of Paonta Sahib (Negi, 1991). It drains predominantly the sandstones of the Siwaliks with minor conglomerates and claystones.

Didar Gad

This stream originates in the Higher Himalaya and drains the Almora Crystallines before joining the Yamuna.

Barni Gad

It drains the chloritic phyllites and blue limestones of Mandhali Formation and dolomitic limestones of Deoban Formation before joining the Yamuna near Kuwa. It draws water from a number of tributaries in its upper reaches.

The Pabar

The Pabar (Fig. 2.5) is a large tributary of the Tons. It rises from the Dhauladhar Range in the Shimla district and is fed by the Chandra Nahan glacier and springs emanating from underground water (Negi, 1991).

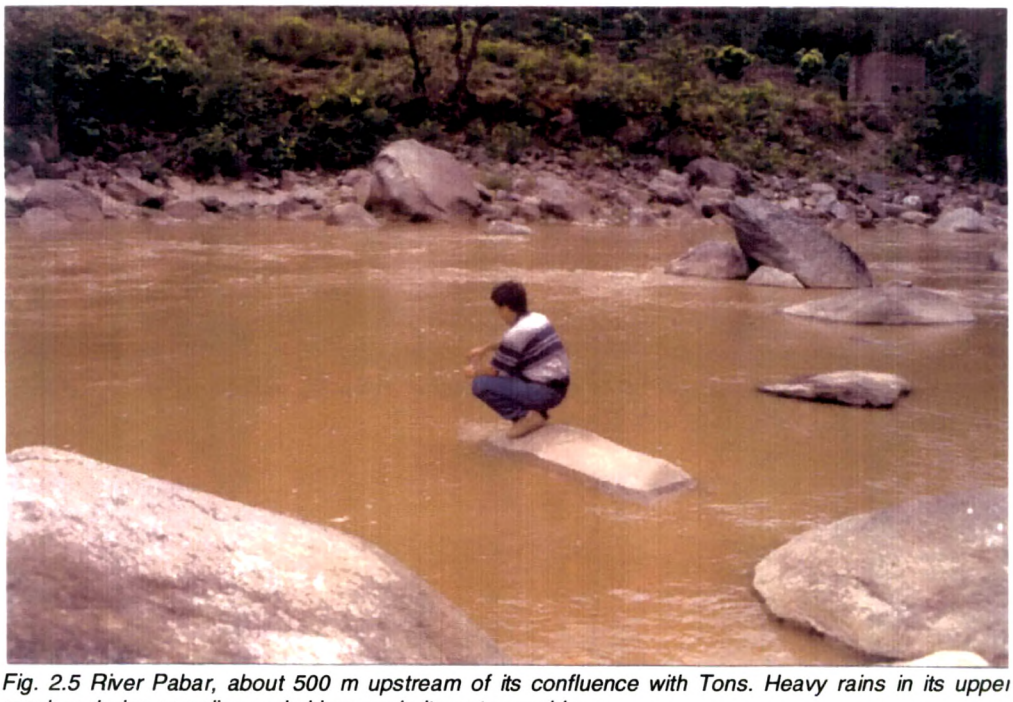

Fig. 2.5 River Pabar, about 500 m upstream of its confluence with Tons. Heavy rains in its upper reaches during sampling period has made its water muddy.

It joins the Tons near Tiuni. In its upper reaches it drains the lithology of the Almora Crystallines, the Ramgarh Group. Downstream it flows through the Nagthat quartzites and greenish gray phyllites and slates alternating with gray-black carbonaceous and pyritous limestones.

Godu Gad

It originates in the Higher Himalaya where it drains the Almora Crystallines (Valdiya, 1980) comprising biotite-rich felspathic schist and bitotite-sericite phyllonite. It flows through massive coarse-grained sercitic quartzite of Berinag Formation before it joins the Tons near Mori.

Shej Khad

It is a tributary of the Tons. Shej Khad drains predominantly the dolomites and dolomitic limestones of Deoban Formation before it joins the Yamuna near Minas.

2.1.2 Climate of the Yamuna catchment

The drainage basins of the Yamuna and its tributaries, covering the northwestern part of the Uttaranchal State (Fig. 2.1, 2.2), experience tropical monsoon climate with much variability introduced by the altitude, mountain barriers, air masses and their movement (Devi, 1992). Altitude and mountain barriers are major factors that regulate much of the variations in the rainfall and temperature in the region. January is the coldest month while the maximum temperature is in the month of June. After June, the temperature decreases with the onset of southwest monsoon with a secondary maximum of temperature in September when there is a sharp drop in the cloudiness in the region. Both diurnal and annual ranges of temperatures decrease from the plains up to the elevations ranging from 2100 to 2400 m, beyond which they again increase. The amount of insolation received along the mountain slopes differs according to the gradient and direction of slopes. South and southwest facing slopes are expected to receive maximum insolation than those facing north and northeast as the sun remains south of the area throughout the year. Fig 2.6 shows the monthly temperature variations in some of the places in the Yamuna catchment. The driest month of April and May have the largest diurnal range and the most humid months July and August have the least. The annual relative humidity in the catchment is about 65 %. Higher relative humidity is observed along the southern slopes of the Himalaya as the monsoon winds are forced to

ascend leading to their adiabatic cooling and condensation of moisture. Therefore, high humidity is observed at Mussoorie, Nainital and Chakrata varying from 85 to 95 % during the monsoon months. The amount of rainfall varies with elevation as well as with the location. Heavy orographic rainfall occurs on the windward side of the ranges with a rapid decrease of rainfall on the leeward side.

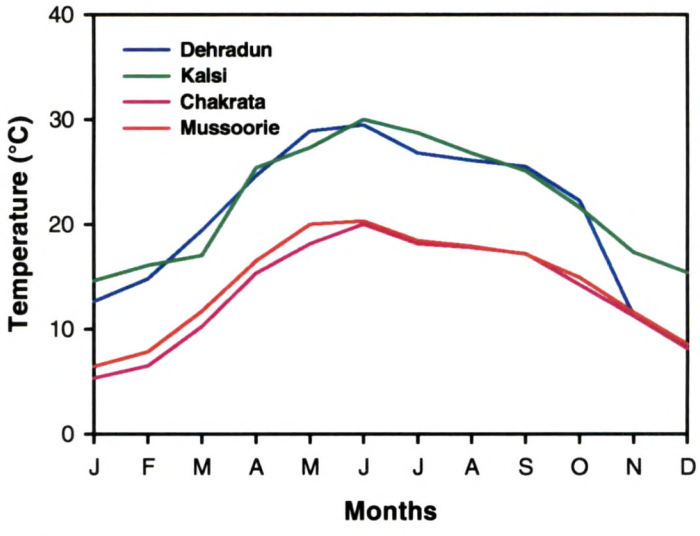

Fig. 2.6 Mean monthly temperature variations in the Yamuna catchment in the Himalaya (Devi, 1992).

The summer rain gradually decreases in amount as one moves along the Himalayan range from east to west. In general, the amount of rainfall increases with elevation except over the northern snowclad areas. The tropical storms and depressions largely influence the local rainfall. Such storms form over the Bay of Bengal and the Arabian Sea and enter the region from southeast and southwest. Heavy rains are associated with slowly moving tropical cyclones due to an increase in the duration of rainfall. The southwest monsoon hits the region around the last week of June and withdraws around the last week of September. The annual rainfall at Dehradun and Kalsi, situated at the foothills of the Himalaya, is ~210 cm whereas in Mussoorie, lying on the windward side of the mountain slope, receives an annual rainfall of ~270 cm. About 80 % of this is contributed by southwest monsoon during July-September (Fig. 2.7). Short duration high intensity rains are common. During monsoon, heavy flood in the Yamuna causes serious damage in the region. Study on peak floods shows that many of them are recorded during late September and early October (Agarwal and Chak, 1991). Occasional heavy rains during these periods, when the catchment is nearly saturated with

water and the river is full, results in floods during this month. Floods in July, August and early September are generally milder. Potential evapotranspiration (P.E.), which represents the water loss in the hydrological cycle, shows large monthly variations in the Yamuna catchment (Fig. 2.7).

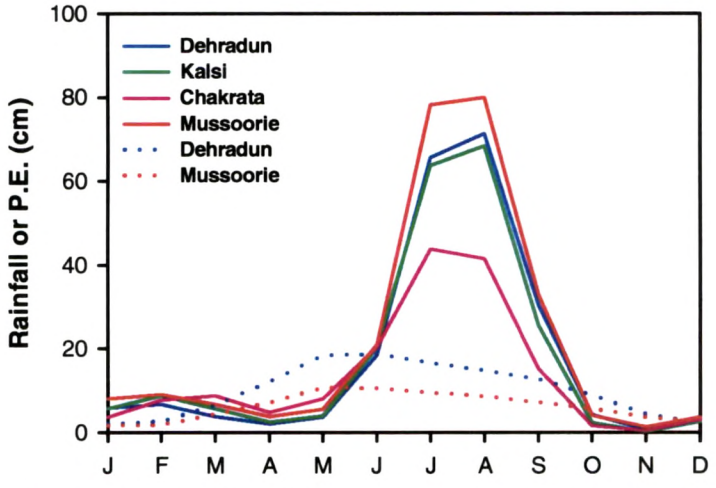

Fig. 2.7 Mean monthly rainfall (solid lines) and potential evapotranspiration (dotted lines) variation at some stations in the Yamuna catchment in the Himalaya (Devi, 1992).

The factors controlling P. E. are temperature, distances from the sea, altitude, characteristics of the rainfall, cloudiness of the sky etc. All these factors form a complex combination influencing the distribution of temperature and consequently the distribution of P.E. over the region. The mean values of P.E. during the summer are five to six folds higher than those during the winter. In the mountain and the foothill regions, during monsoon period, due to higher precipitation and low potential evapotranspiration, the water yield is higher with a large annual variation (Devi, 1992).

Soil formation is governed by the climate (precipitation and temperature), parent lithology, vegetation and gradient in the catchment. The soils in these regions have been grouped as brown-hill soils (Devi, 1992) which form from weathering of granite, gneiss and garnetiferrous and biotitic schist. Based on the pedogenic soil forming processes under the climatic and topographic conditions, four types of soils are found: (i) red loam (in dry places), (ii) brown forest (in surfaces with moderate organic content), (iii) podsol (in humid condition) and (iv) meadow soils (near *nallas* and cool, shady and perennially moist places). Soils on the slopes (15 to 40 percent) are shallow due to erosion and mass wasting processes

(Ghildyal, 1990) and usually have very thin surface horizons. Soil loss in the region varies with the extent of vegetation. Variability in temperature, precipitation and soil thickness also influences the distribution of vegetation in the catchment. Intensive cultivation is observed on terraced hillslopes.

The Yamuna emerges from the hills near Tajewala where the water is taken off by the western and eastern Yamuna canals. The YRS drains an area of about 9600 km^2 in the Himalaya with an annual water flow 10.8×10^{12} liters at Tajewala (Jha et al., 1988, Rao, 1975). About 80% of the water discharge occurs in the month of July, August and September. Monthly variation of water flow in the Yamuna at New Delhi Bridge is given in Fig. 2.8. The total length of the Yamuna from its origin till its confluence with Ganga at Allahabad is 1376 km.

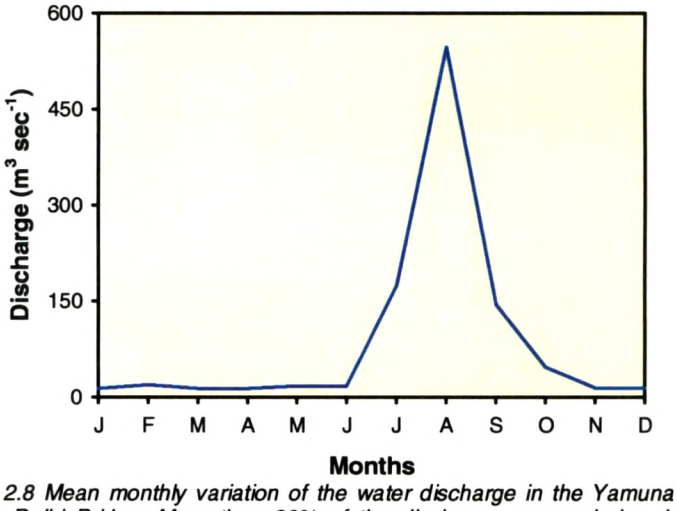

Fig. 2.8 Mean monthly variation of the water discharge in the Yamuna at New Delhi Bridge. More than 80% of the discharge occurs during July, August and September. Data from V. Subramanian (personal communication, 2001)

II. METHODS

To achieve the objectives as outlined earlier, samples of river water, riverbed sediments and various source rocks (granites, carbonates and phosphates) were collected and analyzed for suite of chemical constituents and properties. Details of sampling, sample preparation and analytical techniques are discussed below.

2.2 SAMPLING

(a) River water

Three field campaigns were carried out during October 1998, June and September 1999 corresponding to post-monsoon, summer and monsoon periods respectively (Appendix 2.1). Samples of river water and bed sediments were collected along the entire stretch of the Yamuna and its tributaries in the Himalaya, from near its source at Hanuman Chatti to its outflow at the foothills at Saharanpur (Fig 2.9). In addition, few granite samples were collected from outcrops in and around Hanuman Chatti. Water samples were collected by and large from midstream to avoid local inhomogeneity. Samples were collected in pre-cleaned plastic carboys, which were profusely rinsed with the ambient river water before sampling. About 150 ml of the water was kept in pre-cleaned polyethylene bottles for alkalinity measurements. The remaining water was filtered through 0.4μ Nulceopore® polycarbonate filters within 3-6 hours of their collection. An aliquot of the filtered water of each sample was acidified to pH <2 with ultrapure HNO_3 (Seastar baseline). Acidified samples were stored in acid cleaned HDPE bottles and the unacidified samples in HDPE bottles that were kept in distilled water for several days. Before sample storage, bottles were thoroughly rinsed with filtered river waters. All the sample splits were carried to the laboratory for measurements of various parameters.

For preparation of blanks, double distilled or Milli Q water was passed through Nulceopore® filter papers at sampling site. Acidified and unacidified aliquots of this water were carried to the laboratory to assess the blank contribution resulting from sample processing.

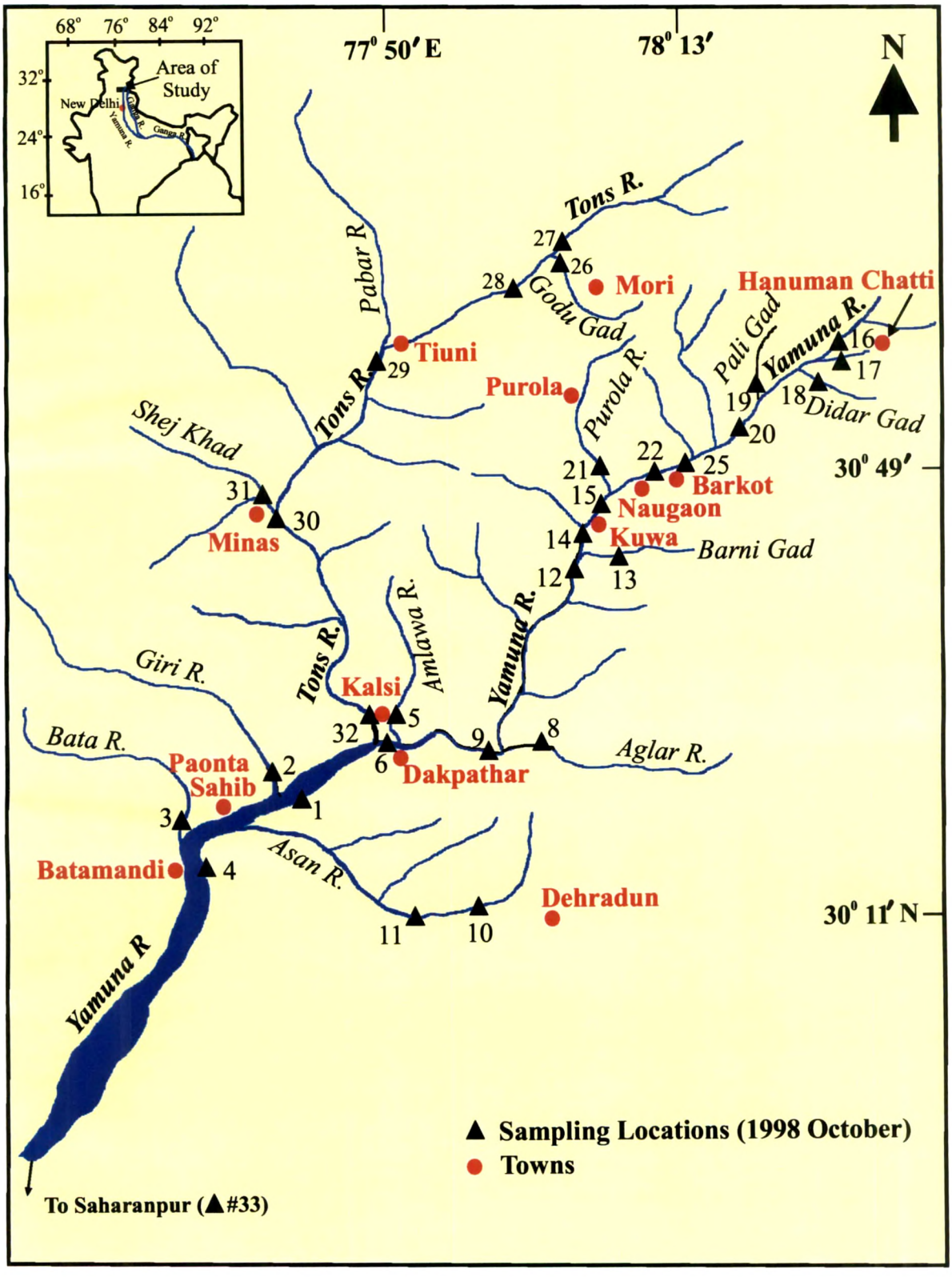

Fig. 2.9 Sampling locations map. Locations are only given for October 1998 collection.

(b) Riverbed sediments

Bed sediments were collected from the midstream as well as from the riverbanks with a plastic scoop and stored in zip-lock polythene bags. In the lab, sample aliquots were dried at ~90°C in an oven and sieved using nylon sieves to less than 1 mm size. The <1 mm size fraction of the sediments were powdered either in a Spex ball mill with acrylic container and methylacrate balls or in an agate mortar, sieved to -100 mesh with nylon sieves. Samples larger than 100 mesh were repeatedly powdered to bring all the materials to -100 mesh size. During powdering care was taken to ensure that the samples did not come in contact with any metal surfaces. After thorough homogenization, powdered samples were stored in clean plastic bottles for elemental and isotopic analyses.

(c) Bed rocks

Granite samples were collected from the outcrops in the Yamuna catchment. Rock masses were broken with a hammer, fresh rocks were chipped and stored in plastic bags. In the laboratory, chunks of fresh rocks were hand picked, pulverized and powdered in agate mortars and sieved to -100 mesh through nylon sieves. Sample powders, after thorough homogenization, were stored in clean plastic bottles for analysis.

Phosphorite samples collected by Singh (1999) from Maldeota and Durmala phosphorite mines were powdered and stored following the procedures outlined above for the bedrocks and granites.

2.3 ANALYTICAL TECHNIQUES

2.3.1 River water

(i) Altitude measurement of sampling locations

Altitudes of the sampling locations were measured using an altimeter (Pretel, Model: ALTIplus K2) only for the summer collection (June 1999). The altitude measurements were made w.r.t. the altitude of RW99-2 site. These measured values were calibrated with the altitude of Hanuman Chatti which was known from maps provided by the U.P. State Department of Tourism. For the monsoon (September 1999) and post-monsoon (October 1998) seasons, the altitude was assigned to those locations from where sampling has been done also during summer.

(ii) pH and temperature

pH of the water samples were measured at site using microprocessor based pocket size pH meter (Eutech Cybernetics Model: pH Scan2) with a precision of ±0.1 pH unit. Prior to the measurement, the meter was calibrated w.r.t. buffer solutions of pH 4, 7 and 9.2, freshly prepared from the buffer capsules (Merck®). It was observed during the field campaigns that the pH measured by dipping the electrode of the meter in the river flow and that measured in the river waters collected in a plastic jug were same within the precision of the instrument.

Temperature was measured in the river waters of summer and monsoon collections using a pocket temperature meter (MA Line) with a precision of ±0.1 °C. The measurements were made by dipping the probe into the river flow. The readings attained steady values within 2-3 minutes.

(iii) Major ions

Alkalinity was measured in unfiltered water samples. In the samples from first campaign (October 1998), alkalinity was measured at site by acid titration using a mixed indicator (Merck®). The samples collected during the next two campaigns were analyzed for alkalinity by both manual titration at the sampling site as well as using an Auto Titrator (Metrohm 702 SM Titrino) using a combined glass electrode and fixed pH end point method. The alkalinity values obtained by auto titrator were found to be about 4% higher (Fig. 2.10). The auto

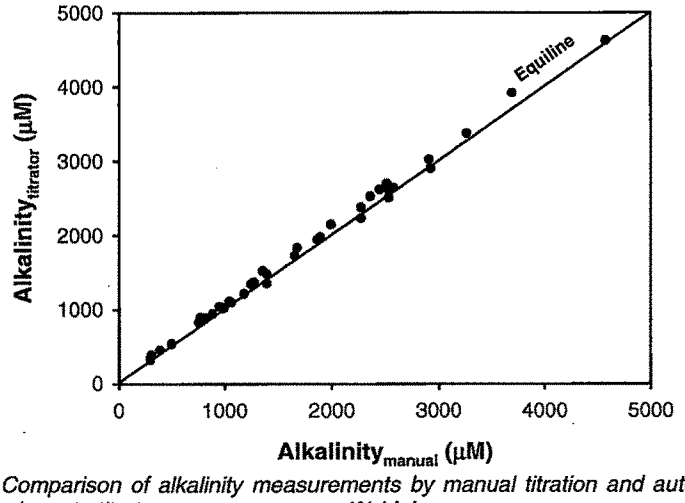

Fig. 2.10 Comparison of alkalinity measurements by manual titration and auto titrator. The values by auto titrator are on average, ~4% higher.

ANALYTICAL SCHEME FOR SAMPLING AND MEASUREMENTS

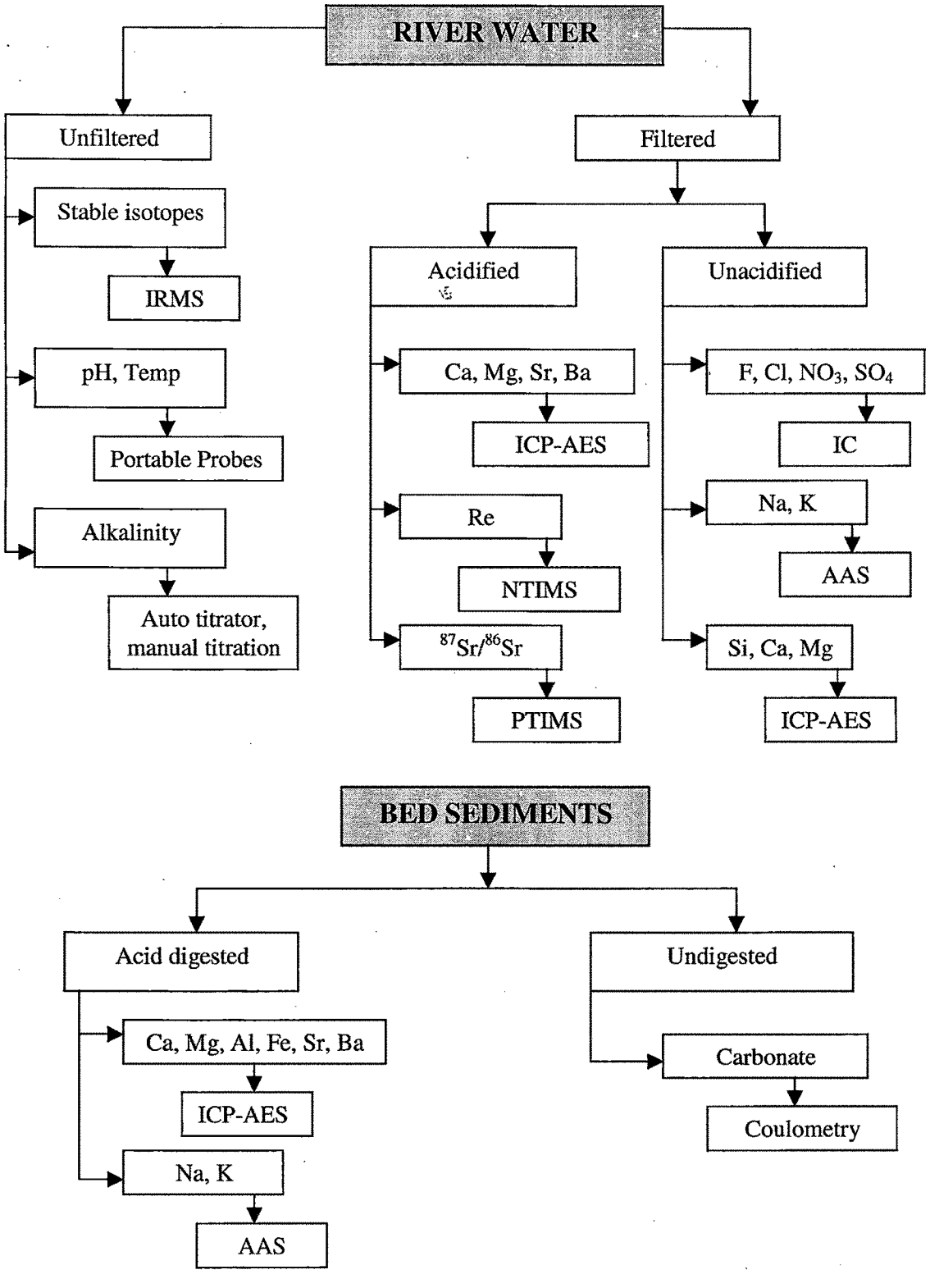

titrator data, for the later two collections, have been accepted and used for all calculations and interpretations. Based on repeat analysis of a number of samples, the reproducibility of alkalinity measurements by auto titrator is ~1% (Appendix 2.2).

Na and K concentrations in the waters were measured by flame-AAS (Perkin Elmer, Model 4000). Calibration was achieved using standard solutions prepared in the laboratory by dissolving analytical grade NaCl and KCl. The concentrated stock solutions were suitably diluted to bring the concentration in the linear analytical range. Based on replicate analysis of the samples, the precision of the measurements are 2.2% and 3.1% for Na and K respectively (Appendix 2.2).

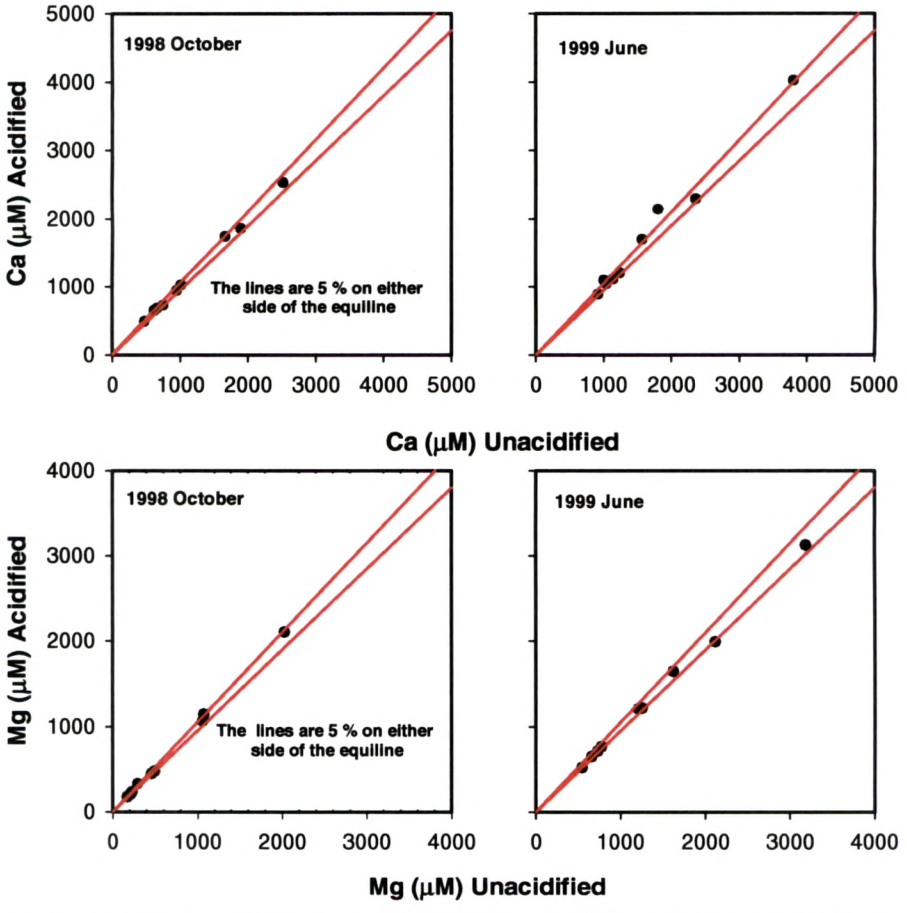

Fig. 2.11 Ca and Mg measurements in unacidified and acidified aliquots of water samples. The concentrations agree within the analytical precision. The analysis was carried out about 10 weeks after sampling.

Si, Ca and Mg were measured by ICP-AES (Jobin Yvon, Model 38S) in unacidified filtered water samples, by sequential scanning of emission lines at wavelengths 251.611, 279.806 and 422.673 nm respectively. The ICP Spectrometer has a Czerny-Turner monochromator of 1 m focal length and 3600 grooves/mm holographic grating with a typical resolution of 0.006 nm, measured w.r.t Cobalt emission line at 228.616 nm. The laboratory standards for Ca, Mg and Si were prepared by dissolving analytical grade $CaCO_3$, pure Mg metal and Na_2SiF_6 respectively. The working calibration curves were generated from these standards. Commercial standards (Merck®) were analyzed on the same calibration lines to check the accuracy of the measurements. At times, the instrument was calibrated w.r.t. commercial standards and elemental concentrations in the laboratory standards were ascertained using these calibration lines. The results of standard analysis for accuracy check are given in the Table 2.1. In a number of water samples, Ca and Mg were analyzed both in the unacidified and acidified filtered aliquots to check on the calcite precipitation, if any, during the period from sampling to analysis. The analysis shows that Ca concentrations in both acidified and unacidified samples were same within the analytical uncertainties (Fig. 2.11) suggesting that over the storage period of 10 weeks, there is no measurable loss of Ca via calcite precipitation in laboratory from these water samples. In addition to analysis of Si by ICP-AES, a number of samples were also analyzed by spectrophotometer using the molybdenum blue method. These data were in good agreement, except in a few samples for which the ICP values were marginally higher. (Fig. 2.12).

F, Cl, NO_3 and SO_4 in the water samples were measured by Ion Chromatography (Dionex series 2000i/SP). The instrument was calibrated w.r.t. standard solutions prepared in the lab from the respective salts (NaF, NaCl, KNO_3 and Na_2SO_4). Cl, NO_3 and SO_4 were separated on a AS4A column using a mixture of 1.8 mM Na_2CO_3 and 1.7 mM $NaHCO_3$ as an eluent, while F was separated on a AS14A column using an eluent of 3.5 mM Na_2CO_3 and 1.00 mM $NaHCO_3$. River waters were analyzed at 10 μS and 30 μS scale whereas rainwater samples were analyzed at 3 μS scale. Check standards of various concentrations were run to check the accuracy and precision of the measurements (Table 2.1). The reproducibility of SO_4 measurements, based on repeat runs of samples is about ±5.4% (Appendix 2.2). The precisions of F, Cl and NO_3 measurements assessed by repeat analysis of standard solutions of varying concentrations (Table 2.1) are better than ±5%. At concentrations less than 0.5 mg

ℓ^{-1}, it is ±10%. The procedural blanks processed at the sampling sites, always produced signals below the detection limits of the instrument (50 µg ℓ^{-1} for F, Cl and NO_3 and 500 µg ℓ^{-1} for SO_4 at 10 µS).

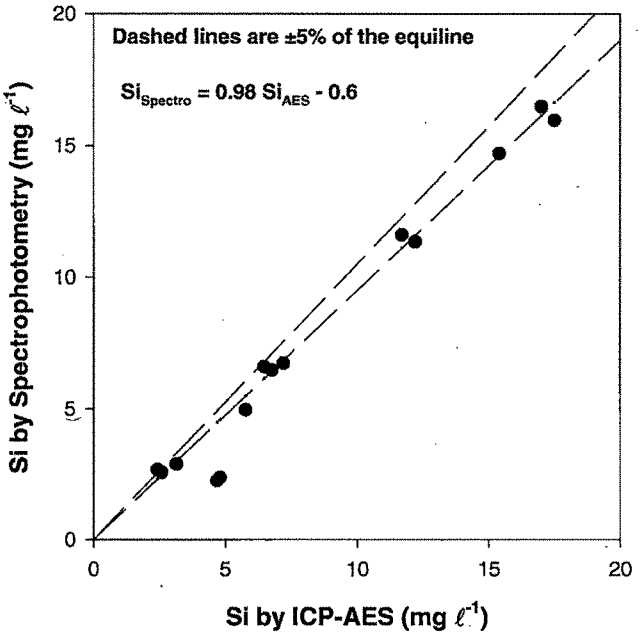

Fig.2.12. Comparison of Si measurement by ICP-AES and spectrophotometry

Table 2.1 Analysis major ions in standards for accuracy check

Parameter	n	Concentration (mg ℓ^{-1})	
		Expected	Measured
Ca	15	10	10.3±0.3
	4	20	20.2±0.7
Mg	15	2	2.05±0.11
	4	4	4.03±0.16
Si	8	8	2.06±0.06
	12	5	5.01±0.18
F	8	0.25	0.24±0.02
	5	0.5	0.48±0.02
	16	1	0.96±0.05
	4	2	2.08±0.06
Cl	7	0.25	0.24±0.03
	5	0.5	0.48±0.04
	17	1	1.03±0.02
	4	2	2.05±0.04
NO_3	14	1	1.02±0.02
	4	2	2.12±0.04
SO_4	4	8	8.44±0.09
	13	20	20.7±0.8

(iv) Strontium and Barium

Sr and Ba concentrations in river water were analyzed in the filtered acidified samples by ICP-AES coupled with a ultrasonic nebulizer (USN). The USN assembly consists of a piezoelectric transducer operating at very high frequency, 1.4 MHz. The water samples are fed by a peristaltic pump onto the face of a quartz plate attached to the transducer. The high frequency oscillations produce fine uniform size aerosols of samples of the size ~10 times smaller than those produced by pneumatic nebulizers. A stream of argon gas then sweeps these aerosols into a heating chamber maintained at 140 °C. The USN is coupled with a desolvation system which consists of a condensation cooler (at ~5 °C) to remove the majority of the solvent (water) aerosols thereby allowing only "dry" aerosols to enter the plasma. This prevents the excessive cooling effect and hence results in improvement of detection limits significantly (Galli and Oddo, 1992; Brenner et al., 1992, Nham, 1992).

Table 2.2 Analysis of Sr and Ba in standards for accuracy check.

Sr ($\mu g\ \ell^{-1}$)				Ba ($\mu g\ \ell^{-1}$)			
n	**Expected**	**Measured**		**n**	**Expected**	**Measured**	
		Mean	**Range**			**Mean**	**Range**
4	5	5.1±0.2	4.9-5.3	5	5	4.8±0.1	4.8-4.9
3	10	9.8±0.2	9.7-10.0	8	10	9.9±0.6	9.0-10.8
13	20	19.8±0.7	18.5-21.3	5	20	19.7±0.5	19.0-20.2

The instrument was calibrated w.r.t. standard solutions prepared from analytical grade salts [$Sr(NO_3)_2$ and $Ba(NO_3)_2$] in the laboratory and the commercial standards (Merck®) were read on these calibration lines. The measured concentrations in the standards agreed with expected values (Table 2.2). The standards were spiked with NaCl solutions to closely match their TDS concentrations with those in river waters. Addition of NaCl in the standards also helps to keep high ionic strength thereby avoiding any possible adsorption of elements onto the walls of the peak tubing of USN. Based on repeat analysis of the samples, the precisions of the measurements are ~3% for Sr and ~5% Ba (Appendix 2.2). Solutions of reference standards G-2 (~6000 times diluted) and W-1 (~3500 times diluted) were analyzed to check the accuracy of the measurements, the results are given in Table 2.3.

Table 2.3 Results of Sr and Ba analysis in reference standards G-2 and W-1.

	G-2 - Measured (μg ℓ^{-1})		W-1 - Measured (μg ℓ^{-1})	
	Sr	**Ba**	**Sr**	**Ba**
	87.8	307	65.7	45.3
	85.2	316	63.5	47.0
	87.9	302	64.7	47.7
	89.4	368	61.2	48.1
Mean measured	***87.6±1.7***	***323±30***	***63.8±1.9***	***47.0±1.2***
Expected[a)]	***80.0***	***315***	***54.3***	***47.1***

[a)]Expected values based on Potts et al. (1992) and dilution of G-2 and W-1 solutions.

(v) Rhenium

Re was measured in waters, granite and carbonate samples. The analytical and measurements scheme of Re measurements in river waters is given in Fig. 4.13. Typically about 100 g of filtered, acidified sample was weighed, spiked with ^{185}Re and stored as such, for at least 24 hours, for sample-spike equilibration. The samples were then dried, digested with ultra pure HNO_3 (Seastar baseline) and taken in 7 ml of 0.8N HNO_3. This solution was loaded onto ion exchange column packed with anion exchange resin (AG1×8, 100-200 mesh). Re was purified through ion exchange in two steps, the first column with a resin volume of 1 ml and the second with 100 μl resin (Trivedi et al., 1999). The resin was loaded onto quartz columns packed with Teflon wool. In the 1ml columns, resin was cleaned with 6N HCl (2 ml twice) and 8N HNO_3 (2 ml thrice), conditioned with 0.8N HNO_3 (3 ml thrice) before loading the sample solution. The columns were washed with 0.8N HNO_3 (3 ml four times) and pure Re was eluted with 8N HNO_3 (4 ml thrice). The eluate was dried, oxidized in conc. HNO_3 and taken in 1ml 0.8N HNO_3. This solution was loaded onto a 100 μl resin column cleaned with 6N HCl (1 ml twice) and 8N HNO_3 (1 ml thrice), conditioned with 0.8N HNO_3 (1 ml thrice). The columns were washed with 0.4N HNO_3 (1 ml thrice) and pure Re eluted in 8N HNO_3 (1 ml thrice).

Pure Re fractions were dried, oxidized with conc. HNO_3 and dissolved in 0.2N HNO_3 during initial phase of analysis and taken in pre-cleaned Teflon tubes attached to a micro syringe. They were loaded and evaporated on high purity degassed Pt filaments (H. Cross

Company, USA). About 10 μg of specpure $Ba(NO_3)_2$ solution was loaded on top of the sample on the Pt filament and put in the mass spectrometer.

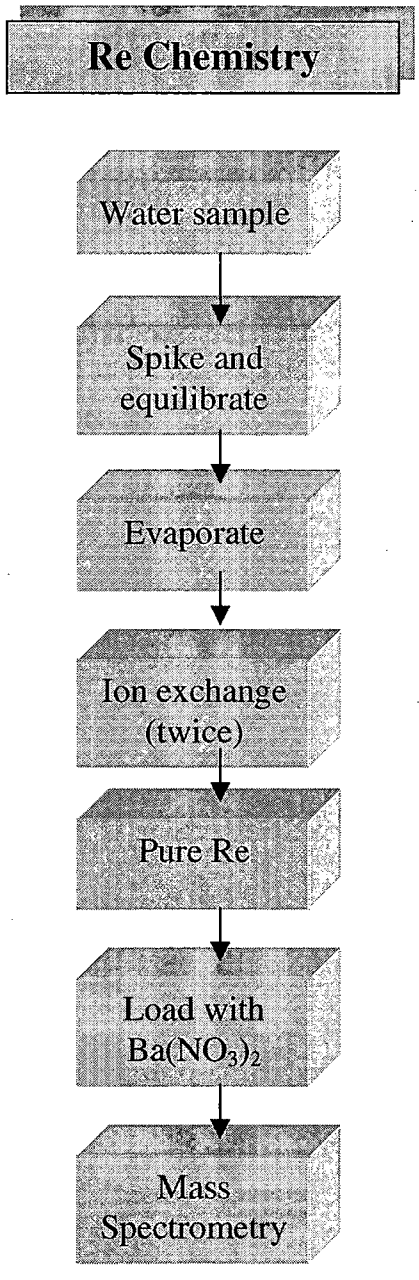

Fig. 2.13 Flow diagram of Re chemistry

It was found that by loading the sample in HNO_3 medium, emission of Re signal was delayed perhaps due to the presence of organic matter. Afterwards, the samples were taken in quartz

distilled water for loading which facilitated the easy emission of the Re signal allowing the samples to be run at a lower temperature than previously done. Re was analyzed in the samples by Negative Thermal Ionization Mass Spectrometry (N-TIMS) following the procedures of Trivedi et al. (1999). Re signal as ReO_4^- was scanned at masses 249 and 251. Corrections for oxide interference were made ($^{185}Re\ ^{16}O_3\ ^{18}O^-$ on $^{187}Re\ ^{16}O_4^-$) to calculate Re concentrations (Trivedi et al., 1999). The ^{185}Re spike used in this study is diluted from the concentrated spike described in Trivedi et al. (1999) and has a strength of 1.193 ng g^{-1}. This spike was calibrated w.r.t. the standard from time to time during the course of the analysis (Table 2.4).

Table 2.4 Re Standard Calibration *(w.r.t. spike ID : 1.193 ng g^{-1})*

Date	N	X±2σ (ng g^{-1})	X±2σ_μ (ng g^{-1})
03/05/99	141	38.22±0.56	38.22±0.05
22/06/99	93	38.49±0.36	38.49±0.04
01/08/99	79	38.48±0.79	38.48±0.09
02/08/99	105	38.30±0.56	38.30±0.05
Weighted mean		***38.40±0.25***	***38.37±0.03***

This value compares with the values of 37.6 ng g^{-1} based on dilution and the 37.22±0.03 ng g^{-1} as measured by Singh (1999). The above results of calibration exclude one run of the standard with a value of 40.53±0.35 ng g^{-1}.

For the chemistry and mass spectrometry followed for Re analysis, all the acids and water used were of ultrapure quality. HNO_3 was procured from Seastar Chemicals Inc., Canada. Commercially available HCl (analytical grade) was purified in the lab first by distilling it at sub-boiling temperatures using a quartz still and then redistilled in a Teflon distillation set-up under an infra red lamp. Commercially available distilled water was first quartz distilled once in the lab to produce double distilled water (DD H_2O) which was redistilled twice in another quartz distillation set-up. This water (QD H_2O) was used for wet chemistry and mass spectrometry. The Teflon wares (vials and beakers) were procured from Savillex Corporation, USA. The vials, beakers and the quartz columns were initially cleaned thoroughly with DD H_2O, boiled in conc. HNO_3 for several hours, rinsed profusely with DD

H_2O and finally with QD H_2O. The Savillex vials were then filled with a cleaning solution of HF, HNO_3 and H_2O in 2:2:1 ratio, sealed, wrapped with cling films in a plastic petri-dish and kept under infra red lamp for several hours to days. The vials were emptied, rinsed several times with DD H_2O and finally with QD H_2O before use.

The blank contribution of Re to the measured signals was ascertained mainly through incremental analysis. In this approach, 3 or 4 aliquots of the same sample, ranging in size between 10-200g were analyzed for Re. The results, when plotted between the weight of sample analyzed vs. the amount of Re measured, yield an intercept which equals the total procedural blank (Fig. 2.14). In addition, independent determination of the Re blank was made by measuring its contribution from the chemical procedure carried out with all the reagents in quantities similar to those used for the samples. The total Re blank in the present study is determined to be 3.7 pg based on 6 sets of incremental analyses and 6 reagent blank measurements (Table 2.5). This value has been used for blank correction. A part of this total Re blank results from the contribution of Re from Pt filaments. This contribution, measured by running Re-spike loaded on Pt filaments with Ba $(NO_3)_2$, was in the range of 0.2 to 1.9 pg at currents same as or marginally higher than those applied during the sample runs. The blank correction in bulk of the samples is less than 5 % of the measured Re signals, only in four of them (out of 60) the correction exceeded 10 %. The precision of Re measurements, based on the several repeat analyses, is better than 5 % ($\pm 2\sigma$, Table 2.6). The range in the Re concentrations in the samples analyzed in this study is much larger than the blank correction and the precision of the measurements. Out of 75 analyses made (river and mine waters), only in 7 the blank correction would exceed 10 % even if an upper limit of 6.5 pg (mean + 1σ) Re blank is used for the correction. This amount of blank correction is much lower compared to magnitude of two orders of variations observed in the dissolved Re concentrations in the Yamuna and its tributaries. Hence the interpretations and conclusions drawn based on these data (Chapter 5) are not affected blank corrections.

Table 2.5 Re blank contribution (pg)

	Procedural	Incremental
	9.25	5.58
	6.50	3.13
	1.69	0.77
	2.48	4.76
	5.96	3.51
	0.88	0.00
Mean (n = 12)	***3.71±2.77***	

Table 2.6 Results of repeat Re analysis (ng ℓ^{-1})

Sample Code	1	2	3
RW98-4	2.71±0.05	2.78±0.05	2.75±0.05
RW98-6	1.10±0.04	1.08±0.02	
RW98-8	3.52±0.17	3.49±0.15	
RW98-13	0.89±0.04	0.81±0.05	0.85±0.05
RW98-16	0.99±0.04	1.02±0.05	1.02±0.02
RW98-21	0.31±0.04	0.31±0.04	
RW98-31	3.49±0.15	3.48±0.05	
RW99-6	1.47±0.01	1.47±0.06	1.40±0.06
RW99-29	1.93±0.08	1.76±0.06	
RW99-53	0.65±0.02	0.62±0.03	0.66±0.03
RW99-59	0.98±0.04	1.01±0.03	1.02±0.06

Errors are ±2σ

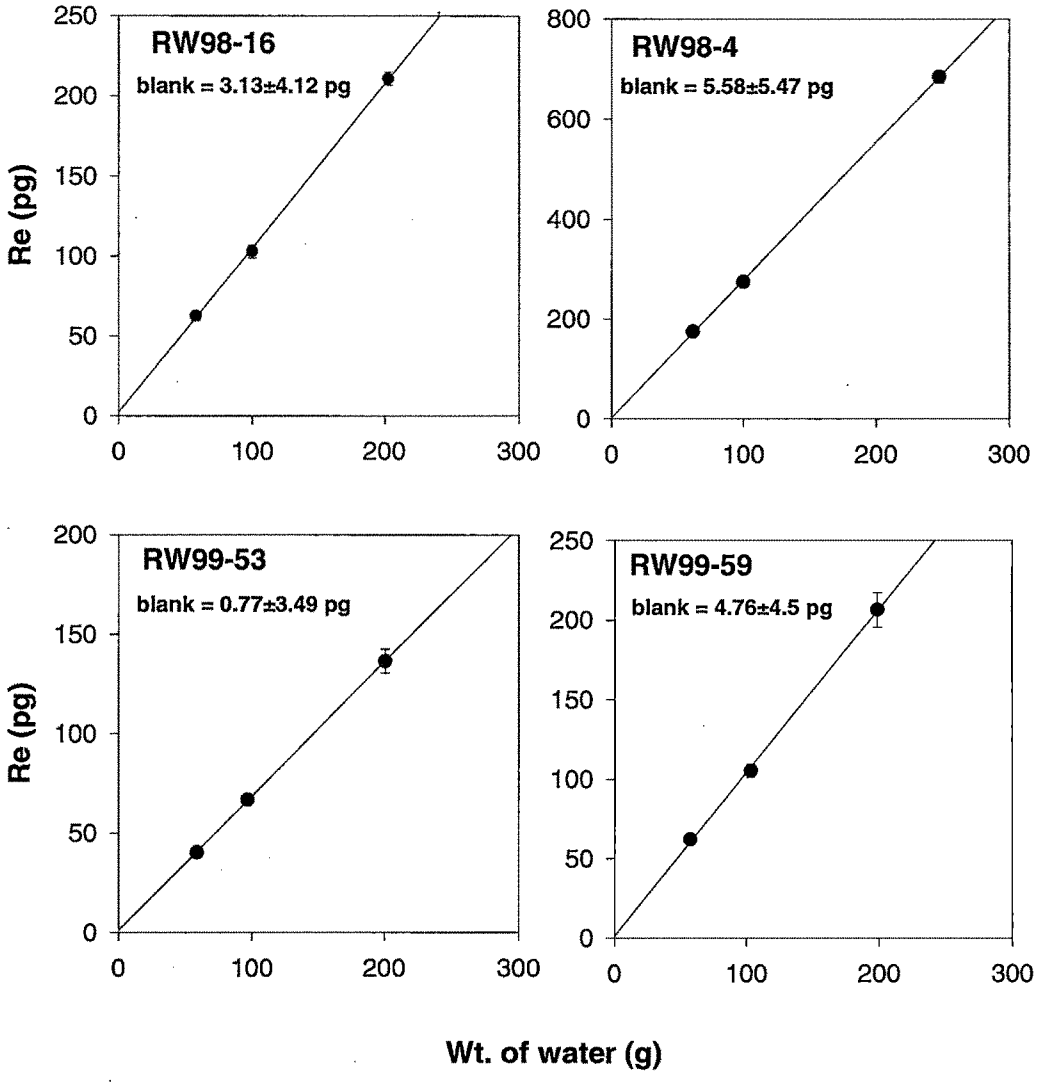

Fig. 2.14 Weight of water analyzed vs. total amount of Re in the sample. The intercept of the regression line gives a measure of the total rhenium blank. The error bars are ±2σ in the Re concentrations.

(vi) Sr isotopes

Sr isotopic abundance were measured in the water and rock samples by a triple collector TIMS (VG 354) at National Geophysical Research Institute, Hyderabad. Sr was separated from Rb and other matrix elements through ion exchange chromatography. The ion exchange columns were made of quartz tubes (ID = 6 mm, OD = 8 mm). The columns were packed with cation exchange resin (Dowex 50X8, 200-400 mesh) to a height of 16 cm. About 50-150 mℓ of water samples were taken in FEP beakers and were kept on a hot plate for drying (these volumes were decided, based on Sr concentration, to yield at least 1 μg Sr load). At incipient dryness, few drops of conc. ultrapure HNO_3 was added and the samples were then dried completely. To this dilute quartz distilled (QD) HCl was added and the samples were dried. This procedure was repeated to ensure complete chloride conversion of Sr in the samples. The dried samples were taken in 1.5 mℓ 2N QD HCl and centrifuged for about 5 minutes in 3 mℓ quartz centrifuge tubes. During centrifugation, the tubes with the samples were covered with parafilms. The supernatant solution was loaded on to the resin column (pre-cleaned with 6N HCl and conditioned with 2N HCl) using a quartz pipette. The walls of the column of reservoirs were washed with 0.5 mℓ 2N HCl twice after the sample solutions passed through completely. The columns were washed with 2N HCl (about 7 times the column volume) before the pure Sr fractions were eluted (with 2N HCl). The pure Sr fractions were collected in 15 mℓ round bottom Savillex vials, evaporated to dryness and stored for analysis. After every sample, the columns were cleaned with about 40 mℓ 6N HCl and 20 mℓ QD water and conditioned with about 25 mℓ 2N HCl. The columns were calibrated from time to time especially when a new batch of acid was used.

The pure Sr fractions were dissolved in 0.5N HNO_3, taken in pre-cleaned Teflon tubes and loaded and evaporated directly on degassed high purity Ta filaments already loaded with H_3PO_4. Sr isotopic measurements were carried out both in single as well as triple collector mode. During the period of analysis SRM 987 standard was run a number of times which yielded an error weighted $^{87}Sr/^{86}Sr$: 0.710184±0.000006 (2σ, n = 9). Some samples were processed in replicate and analyzed for their isotopic abundance. The results of the repeat analyses are given in Table 2.7. Few samples were run twice to check the instrument performance and a few were run both in single as well as triple collector mode (Table 2.7).

Procedural blanks were assessed by processing the distilled water filtered at sampling site and the reagents used for the sample processing. Based on six runs, the blanks for the present study centered at 3.6±0.8 ng. $^{87}Sr/^{86}Sr$ in the blanks were not measured and hence $^{87}Sr/^{86}Sr$ in the samples were not corrected for blank contributions. Using the amount of sample Sr load and assuming $^{87}Sr/^{86}Sr$ to be 0.7 in the blank, it can be calculated that measured $^{87}Sr/^{86}Sr$ will be altered at 10^{-4} only in four of 55 samples analyzed.

Table 2.7 Repeat measurements of Sr isotopes

Sample	Run-I	Run-II
RW98-2[a)]	0.71920 (3)	0.71929 (1)
RW98-11[a)]	0.71491 (3)	0.71491 (5)
RW99-29[a)]	0.72292 (1)	0.72304 (1)
RW99-58[a)]	0.73446 (1)	0.73445 (2)
RW99-63	0.72835 (5)[b)]	0.72840 (1)[c)]
RW99-64	0.73317 (4)[b)]	0.73316 (4)[c)]
RW99-13	0.75548 (2)[d)]	0.75543 (2)[e)]
RW99-29R	0.72307 (1)[d)]	0.72304 (1)[e)]

[a)]processed and run in duplicates, [b)]run in single collector, [c)]run in triple collector, [d)]first run in triple collector, [e)]second run in triple collector. The numbers in the parentheses indicate error on the last decimal places (±1σ).

***(vii) Stable isotopes*:**

The oxygen and hydrogen isotope measurements were carried out on unfiltered water samples using a water equilibration system and GEO 20-20 mass spectrometer (PDZ Europa, U.K.). 1 ml of water sample was pipetted into a glass bottle with airtight stopcock, equilibrated with tank CO_2 (35°C, 12 hours) for oxygen and tank H_2 (35 °C, 12 hours in presence of platinum catalyst) for hydrogen. Aliquots of equilibrated CO_2 and H_2 were cryogenically separated (Epstein and Mayeda, 1953; Brand et al., 1996). The flushing, filling and sampling of gases were done using a Gilson auto sampler controlled by the mass spectrometer software. The isotopic compositions of CO_2 and H_2 were analyzed following standard IRMS procedures (Allison et al., 1995). Along with each batch of samples, a laboratory water standard (NARM, Narmada River Water, $\delta^{18}O$ = -4.52‰, δD = -35.2‰) was also measured using which the final sample δ-values (w.r.t. V-SMOW) were calculated. The overall precision, based on repeat measurements of about 16 samples, is ±0.1‰ for $\delta^{18}O$

and ±1.2‰ for δD (Fig. 2.15). For δD, two sets of repeat analysis showed significant difference, ~4‰ each. Excluding these runs, the precision of δD becomes ~0.8‰.

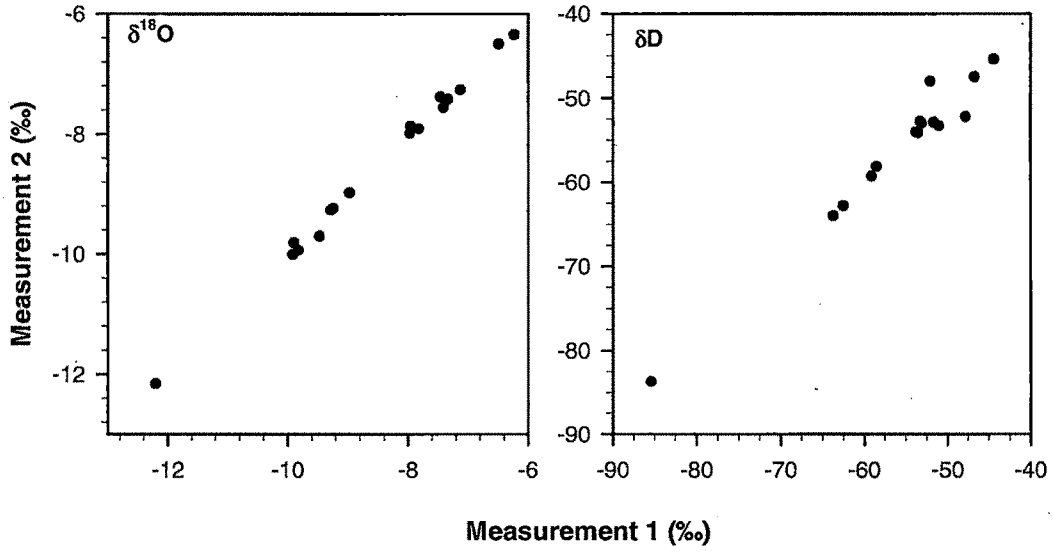

Fig. 2.15 Repeat measurements of $\delta^{18}O$ and δD in river water samples

2.3.2 Rocks and bed sediments

(i) Dissolution

~500 mg of powdered sample (bed rock/granite) was weighed and dissolved in PTFE dish with HF-HCl-HNO_3-$HClO_4$ mixture. For some samples, it was necessary to centrifuge the sample-reagent mixture and attack the residue afresh with the acids. The final solution was taken in 1N HCl and made up to a known volume. These were used for elemental analysis after suitable dilution wherever necessary. USGS rock standards (G-2 and W-1) were also dissolved along with the samples. Reagents used in the sample dissolution procedure were taken to assess the blank concentration from reagents.

(ii) Major ions

Ca, Mg, Al, Fe in bedrock samples were measured by ICP-AES. The instrument was calibrated with laboratory standards prepared as: Ca from $CaCO_3$, and Mg, Al and Fe from pure metals. The USGS standard G-2 and commercial standard solution (Merck®) were run on the same calibration curves. Na and K in the acid digested samples were measured by flame AAS. Standards for calibration were prepared in the laboratory by dissolving analytical

grade NaCl and KCl salts. Mixed or single working standards were prepared in the range of 2 to 10 mg ℓ^{-1} for Na and 1 to 10 mg ℓ^{-1} for K to generate linear calibration curves. Accuracy of the measurements was checked by analyzing the concentrations of major ions of reference standard G-2 on the same calibration curve. Measured concentrations agreed well with the reported values (Table 2.8, Fig. 2.16). Reagent blanks always produced signal negligibly small compared to the sample signals. Few samples, dissolved in replicates, were run to check the reproducibility of the major ion measurements in the bed sediments (Fig. 2.17).

Table 2.8 Results of major ion analysis in reference standard G-2

Element (%)	Reported[a)] (%)	Measured (%)
Na	3.02	3.02
K	3.73	3.66
Ca	1.41	1.39
Mg	0.46	0.46
Al	8.01	8.02
Fe	1.85	1.82

[a)]Reported values from Potts et al. (1992)

(iii) Strontium and Barium

Sr and Ba in the bed sediments were measured by ICP-AES coupled with the pneumatic nebulizer. W-1 dissolved along with the samples were run in the calibration line made from the solution of G-2. Sr and Ba concentrations measured in W-1 were in good agreement with the reported values (Table 2.9)

Table 2.9 Sr and Ba analysis in reference standard W-1 (pneumatic nebulizer)

Run#	Sr (ppm)	Ba (ppm)
1	190	151
2	205	163
3	181	154
4	187	156
4	202	169
6	189	154
Mean	***192±8***	***158±6***
Reported[a)]	***187***	***162***

[a)]Reported values from Potts et al. (1992)

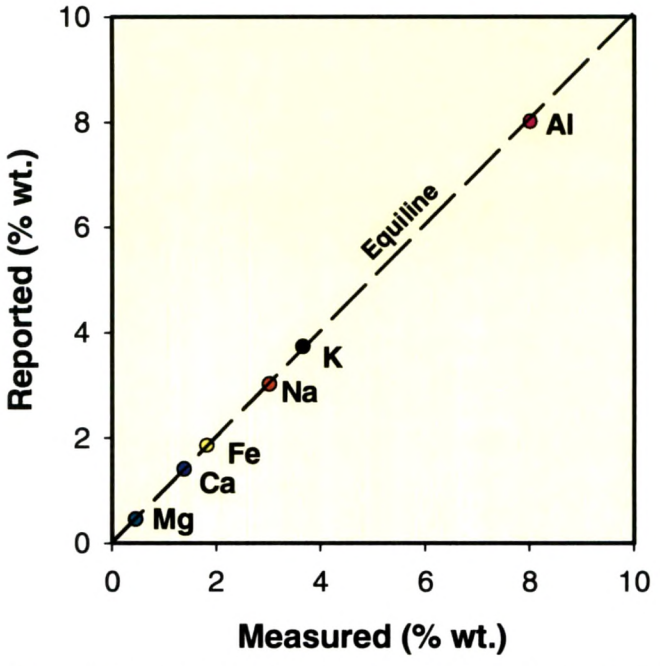

Fig. 2.16 Comparison of measured and reported (Potts et al., 1992) elemental concentrations in the reference standard G-2.

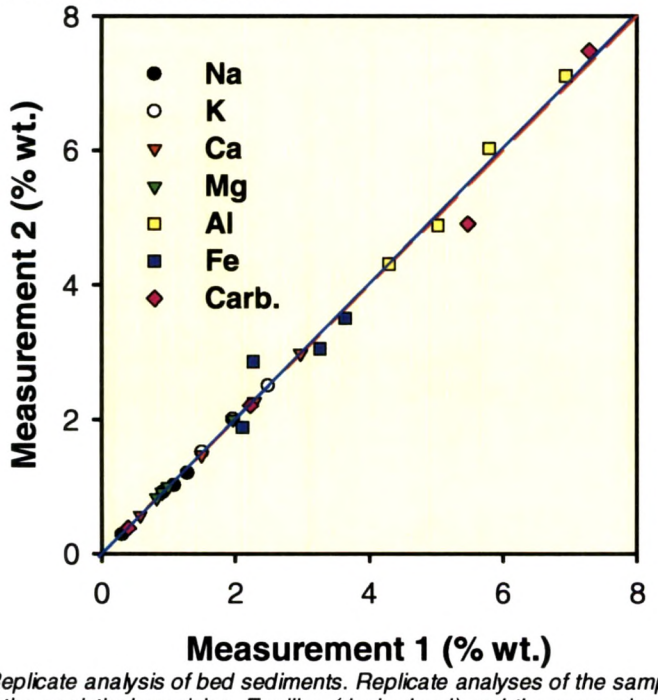

Fig. 2.17 Replicate analysis of bed sediments. Replicate analyses of the samples agree well within the analytical precision. Equiline (dashed red) and the regression line (solid blue) overlap on each other.

(iv) Carbonate contents

Carbonate contents in the bedrocks and granites were measured by Coulometric method (UIC Coulometer, Model: 5012). The analytical calibration was carried with standard solutions made from pure Na_2CO_3 salts dried in oven for 8-10 hours. CO_2 was evolved from ~10-100 mg of powdered sediment/granite samples by treating them with 40% orthophosphoric acid for 10 minutes at 70 °C in an extraction unit in the Coulometer. Compressed air stripped of CO_2 (by passing the air through a 50 % KOH solution) was used as a carrier gas. The liberated CO_2 from the samples was swept by the carrier gas and dried by passing through a column of activated silica gel and anhydrous $MgClO_4$. The dried CO_2 was then passed through the coulometer titration cell. Carbonate contents in the bed sediments were calculated assuming that all CO_2 is from $CaCO_3$. Considering the abundance of dolomites in the catchment (Valdiya, 1980) and high Mg measured in some of the bedrock samples it is likely that part of the carbonates is dolomites. Some samples were run in replicates based on which the reproducibility of the measurement was ascertained to be better than 4 % (Appendix 2.2, Fig. 2.17).

Appendix 2.1

Rivers, locations and seasons of sampling, pH and temperature of the water samples.

Code	River	Location	Drainage Basin[a)]	Season[b)]	pH	Temp. (°C)
Yamuna mainstream						
RW98-16	Yamuna	Hanuman Chatti	HH	PM	8.3	
RW99-13	Yamuna	Hanuman Chatti	HH	S	8.7	10.2
RW98-20	Yamuna	D. of Pali Gad Bridge	LH	PM	8.4	
RW98-25	Yamuna	Barkot	LH	PM	8.7	
RW99-19	Yamuna	Barkot	LH	S	8.9	19.4
RW99-17	Yamuna	Kuthnaur village	LH	S	8.5	15.7
RW98-22	Yamuna	U. of Naugaon	LH	PM	8.7	
RW99-18	Yamuna	Near Lakhmandal	LH	S	9.2	20.2
RW98-15	Yamuna	U. of Barni Gad's confluence	LH	PM	8.7	
RW98-14	Yamuna	D.of Barni Gad's confluence	LH	PM	8.9	
RW99-11	Yamuna	D.of Barni Gad's confluence	LH	S	9.1	21.1
RW98-12	Yamuna	D. of Nainbag	LH	PM	8.6	
RW98-9	Yamuna	D. of Aglar's confluence	LH	PM	8.7	
RW99-51	Yamuna	D. of Aglar's confluence	LH	M	8.6	18.1
RW98-6	Yamuna	U. of Ton's confluence	LH	PM	8.7	
RW99-30	Yamuna	U. of Ton's confluence	LH	S		
RW99-64	Yamuna	U. of Ton's confluence	LH	M	8.4	22.1
RW99-31	Yamuna	D. of Ton's confluence	LH	S	8.4	26.9
RW99-53	Yamuna	D. of Ton's confluence	LH	M	8.5	20.6
RW98-1	Yamuna	Rampur Mandi, Paonta sahib	LH	PM	8.6	
RW99-2	Yamuna	Rampur Mandi, Paonta sahib	LH	S	8.6	21.9
RW99-58	Yamuna	Rampur Mandi, Paonta sahib	LH	M	8.4	20.6
RW98-4	Yamuna	D. of Bata's confluence	LH	PM	8.4	
RW99-5	Yamuna	D. of Bata's confluence	LH	S	8.9	25.9
RW99-55	Yamuna	D. of Bata's confluence	LH	M	7.7	27.5
RW98-33	Yamuna	Yamuna Nagar, Saharanpur	LH	PM	8.4	
RW99-7	Yamuna	Yamuna Nagar, Saharanpur	LH	S	8.7	30.5
RW99-54	Yamuna	Yamuna Nagar, Saharanpur	LH	M	8.2	24.1
Tributaries						
RW98-17	Jharjhar Gad	Hanuman Chatti-Barkot Road	HH	PM	8.2	
RW98-18	Didar Gad	Hanuman Chatti-Barkot Road	HH	PM	8.0	
RW99-14	Didar Gad	Hanuman Chatti-Barkot Road	HH	S	8.3	12.7
RW98-19	Pali Gad	Pali Gad Bridge	HH, LH	PM	8.4	
RW99-16	Pali Gad	Pali Gad Bridge	HH, LH	S	8.1	18.3
RW99-15	Bajri Gad	U. of the bridge over it	LH	S	8.4	13.7

RW98-13	Barni Gad	Kuwa	LH	PM	9.2	
RW99-12	Barni Gad	Kuwa	LH	S	9.1	29.7
RW98-23	Oli Gad	Kuwa-Kapnol Road	LH	PM	8.7	
RW98-21	Purola	Between Naugaon and Purola	LH	PM	8.7	
RW99-20	Purola	Purola-Naugaon Road	LH	S	9.1	21.1
RW98-24	Gamra Gad	Near the bridge over it	LH	PM	8.7	
RW98-26	Godu Gad	Purola-Mori Road	HH, LH	PM	8.3	
RW99-21	Godu Gad	Purola-Mori Road	HH, LH	S	8.8	22.9
RW99-27	Pabar	U. of confluence with Tons	HH, LH	S	7.9	19.9
RW98-27	Tons	Mori	HH	PM	8.1	
RW99-22	Tons	Mori	HH	S	8.4	14.4
RW98-28	Tons	D. of Mori	LH	PM	7.9	
RW99-26	Tons	Before Pabar joins	LH	S	8.0	16.7
RW98-29	Tons	Tiuni	LH	PM	8.0	
RW99-28	Tons	Tiuni	LH	S	7.8	17.7
RW98-31	Shej Khad	Minas	LH	PM	8.6	
RW99-23	Shej Khad	Minas	LH	S	8.7	24.2
RW99-25	Tons	Before Shej Khad joins	LH	S		
RW98-30	Tons	Minas, after confluence	LH	PM	8.4	
RW99-24	Tons	Minas, after confluence	LH	S	8.7	23.4
RW98-5	Amlawa	Kalsi-Chakrata Road	LH	PM	8.6	
RW99-62	Amlawa	Kalsi-Chakrata Road	LH	M	8.4	23.8
RW98-32	Tons	Kalsi, U. of confluence	LH	PM	8.7	
RW99-29	Tons	Kalsi, U. of confluence	LH	S	9.0	27.8
RW99-63	Tons	Kalsi, U. of confluence	LH	M	8.5	21.3
RW98-8	Aglar	U. of Yamuna Bridge	LH	PM	8.8	
RW99-10	Aglar	U. of Yamuna Bridge	LH	S		
RW99-52	Aglar	U. of Yamuna Bridge	LH	M	8.5	22.4
RW98-2	Giri	Rampur Mandi	LH, SW	PM	8.4	
RW99-3	Giri	Rampur Mandi	LH, SW	S	8.5	27.8
RW99-57	Giri	Rampur Mandi	LH, SW	M	8.3	26.6
RW98-3	Bata	Bata Mandi	LH, SW	PM	8.5	
RW99-4	Bata	Bata Mandi	LH, SW	S	8.9	27.4
RW99-56	Bata	Bata Mandi	LH, SW	M	7.9	27.8
RW98-10	*Tons*	*Tons Pol*, Dehradun	LH	PM	8.6	
RW99-65	*Tons*	*Tons Pol*, Dehradun	LH	M	8.4	25.3
RW98-11	Asan	Simla Road Bridge	LH, SW	PM	8.3	
RW99-1	Asan	Simla Road Bridge	LH, SW	S	8.3	26.6
RW99-61	Asan	Simla Road Bridge	LH, SW	M	7.9	27.4
Ganga						
RW98-34	Ganga	Rishikesh	LH	PM	8.6	
RW99-6	Ganga	Rishikesh	LH	S	8.4	15.7

RW99-59	Ganga	Rishikesh	LH	M	8.4	18.6
RW99-8	Bandal	Near Maldeota	LH	S		
Springs						
RW98-7	Kemti Fall	Dehradun-Mussourie Road	LH	PM	8.2	8.2
RW99-9	Kemti Fall	Dehradun-Mussourie Road	LH	S		
RW99-60	Spring	Shahashradhara	LH	M	7.1	7.1

[a] LH: Lesser Himalaya, HH: Higher Himalaya. [b]PM: post-monsoon, S: summer, M: monsoon..

Appendix 2.2 Coefficients of variation for properties measured

Based on duplicate analysis of a number of samples, the coefficients of variation for various measurements were calculated using the formula:

$$CV(\%)=\left[\frac{1}{2n}\Sigma\left(\frac{d_i}{x_i}\right)^2\right]^{\frac{1}{2}}\times 100$$

where d_i is the difference between the duplicates with mean x_i and n is the total sets of duplicates analyzed.

ELEMENT	N	COEFF. VAR (%)
Na	15	2.21
K	14	3.09
Ca	33	4.39
Mg	33	4.85
Alk.	8	1.04
SO_4	15	5.36
Carb.	5	3.67
Sr	15	2.71
Ba	11	4.64

N = number of repeat measurements. The results of major ions, Sr and Ba are in water samples and carbonates in bed sediments.